Synthesis and Structure of Polymer/Metal Interfaces: a Convergence of Views between Theory and Experiment

Christophe Bureau[a]** and Joseph Delhalle[b]

a. Commissariat à l'Energie Atomique, DSM-DRECAM-SRSIM, bât.466, F-91191 Gif-sur-Yvette Cedex (France).

b. Facultés Universitaires Notre-Dame de la Paix, Rue de Bruxelles 61, B-5000 Namur (Belgium).

**E-mail: christophe.bureau@cea.fr

(Received December 10, 1998; accepted April 10, 1999)

Upon performing, under well defined conditions, the electrolysis of organic solutions containing vinylic polymerizable monomers, one can make "hairs" of polymers grow one the surface of the electrodes. The objects obtained by this synthesis constitute true chemical curiosities. Significant contributions from our group are reviewed, which show that the polymer chains are chemically bound to the surface by carbon/metal bonds, and that the thickness and the grafting ratio of the polymer film can be monitored thanks to the electrochemical nature of the initiation steps. These features have motivated many interesting applications in various fields, such as corrosion, adhesion, lubrication or medical surgery, for which the type of the polymer to be grafted (and hence the starting monomer) could be chosen, and the nature of the polymer/metal interface monitored. A detailed overview of the very molecular mechanism of the reactions occuring at the metal/solution interface thus had to be obtained. These mechanisms are very complex, as they involve several competitive paths in solution and on the surface. Some of our contributions in this area are reviewed, focusing on the benefits of a peculiarly strong coupling between surface analysis and theoretical models making use of quantum mechanics on real systems.

1. Introduction

Vinylic monomers such as acrylonitrile (AN) [1], methacrylonitrile (MAN) [2], N-vinyl pyrrolidone (NVP) [3] or methyl-methacrylate (MMA) [4] (Fig. 1) undergo an electropolymerization reaction at metallic electrodes, when submitted to an electrolysis in an anhydrous organic medium (Figs. 2). One significant feature of this synthesis is that two distinct types of polymers are obtained as products of reaction: (i) a physisorbed polymer which can easily be removed by rinsing with a proper solvent (e.g. acetonitrile for PolyMethAcryloNitrile (PMAN)) [5], and which can be up to several micrometers thick [6] depending on the potential scanning protocol during the synthesis ; and (ii) a so-called "grafted" polymer, which is not removed from the metallic surface by rinsing, even under sonication, and which is never thicker than a few hundred Angströms [1,2].

The obvious difference between the two types of polymers is illustrated inFig. 3, in which the thickness of electropolymerized PMAN coatings are measured by ellipsometry, and reported as a function of various

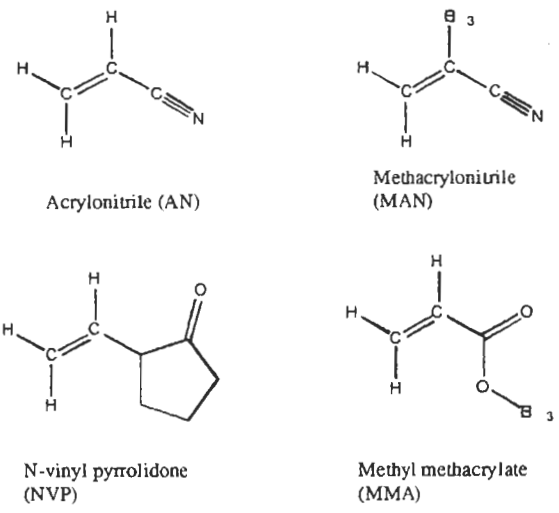

Figure 1 Molecular structures of various polymerizable monomers used for electropolymerization reactions. AN, MAN and MMA are electropolymerized cathodically, while NVP is used at the anode.

This paper is dedicated to Dr. Gérard Lécayon for his retirement, and in honor of his pioneering contributions to the achievement and study of the grafting of polymers onto metallic surfaces.

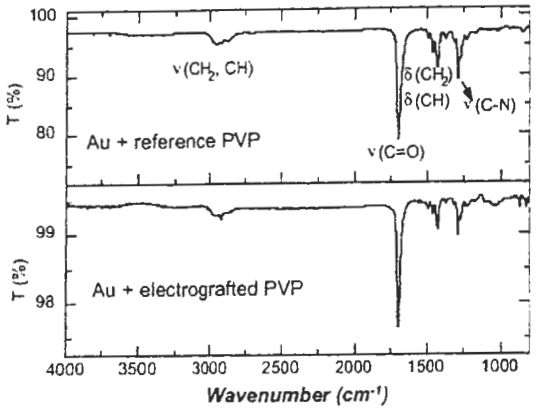

Figure 2 Infra-Red spectra (under Reflexion Absorption Spectroscopy (RAS) conditions) of commercial Poly-Vinyl Pyrrolidone (PVP) spin coated on gold (top), and of a gold electrode PVP film electrografted on a gold electrode. Note the absence of defects in the electrografted film.

rinsingprocedures [7]. Let us first recall that PMAN is insoluble in its monomer (MAN), but highly soluble in acetonitrile (CH_3CN) and acetone.

Fig. 3a illustrates that of a global PMAN coating of about 95 nm (obtained by electropolymerization in *pure* MAN), more than 85 nm are eliminated upon rinsing with acetone, hence pointing to a physisorbed PMAN layer. Only the first 10 nm, which are not removed even under sonication, constitute the remaining grafted polymer. Fig. 3b illustrates the fact that if the electropolymerization is now performed in a solution containing only 20 % of acetonitrile in MAN, then only a thin layer of about 10 nm is directly obtained. These 20 % acetonitrile were sufficient to solubilize the physisorbed polymer, but not to eliminate

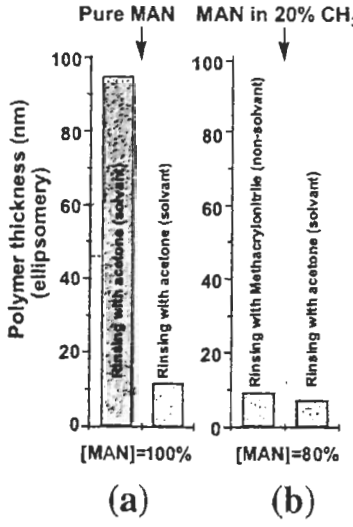

Figure 3 Solubility properties of electrolytic medium against Poly-MethAcryloNitrile (PMAN).

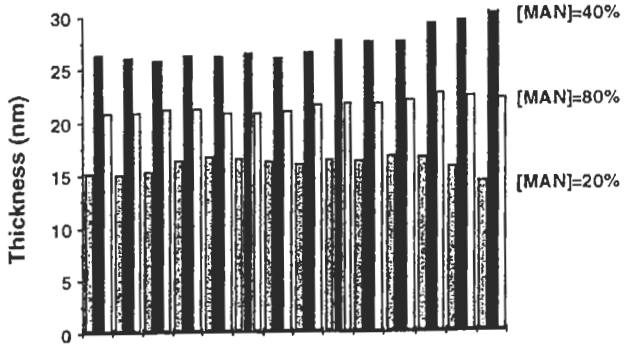

Figure 4 Profiles of thicknesses along a diameter of the RDE polarised in a solution containing 20, 40 and 80% of methacrylonitrile

the underlying grafted film. Note that the thickness of this film remains unchanged upon further rinsing with acetonitrile or acetone, even under sonication, and is identical to that of Fig. 3a [7].

The fact that a grafted polymer film is found on the surface whatever the solubilizing nature of the solution used for the synthesis, suggests that it is obtained directly via surface chemical reaction. One shall note that the alternative hypothesis of a crosslinked (and hence insoluble) polymer precipitating on the surface has been previously considered [8]. However, recent TOF-SIMS experiments carried out on PNVP have demonstrated that the grafted polymer is not crosslinked [9] .

The intuition of a reaction starting from the surface is further qualitatively confirmed by the fact that one can even obtain the above grafted film on the surface of a Rotating Disk Electrode (RDE), spinning at very high rotation rate, say $\omega = 10000$ rpm. At such a high rate (which corresponds to that of the engine of a formula 1 car at start), drastic stirring conditions are forced in the vicinity of the metallic surface : a rough estimation by Navier-Stokes equations reveals that centrifugal velocities of several cm/s are reached even a few nanometers above the rotating surface [7]. One finds that the grafting process is essentially insensitive to such experimental conditions [7] : a grafted PMAN film is present at the end of the synthesis, and its thickness is of the same order of magnitude (*i.e.* a few tens of nm) as for the films obtained at $\omega = 0$ rpm (Fig. 4) [7].

Additionaly, recent experiments in which the electropolymerization is performed on the metallized crystal of a quartz microbalance, reveal that grafted PMAN or PNVP layers are rigidly attached to the surface as they are formed (the notion of rigidity being meant is the sense of the Sauerbrey equation [10]) [11]. However, a simultaneous and in-situ measure of both the eigenfrequency (Df) and of

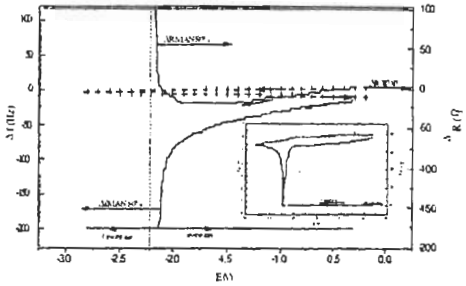

Figure 5 Simultaneous plots of the quartz frequency variation (⟵) and the quartz resonant resistance intensity variation ΔR (—) vs. potential (Ag^+/Ag) during the first cyclic voltammetric experiment in a solution containing MAN (80 vol.%) in acetonitrile (20 vol.%) at a scan rate of 20 $mV.s^{-1}$. Plot of the quartz resonant resistance intensity variation recorded for a solution containing TEAP only (+++) is reported on the graph for comparison. The dots line (.....) indicates the position of the voltammetric peak maximum. Inset : Simultaneous plots of the reduction current (-—) and the whole quartz resonant resistance intensity variation(⟵) vs. potential (Ag^+/Ag) for a solution containing MAN (80 vol.%) in acetonitrile (20 vol.%).

the equivalent resistance changes (DR) of the quartz crystal indicates that the coating which is being built on the surface in the course of the voltammetric experiment is actually rigid only over a limited range of electrode potentials, namely before the voltammetric peak (Fig. 5). At and over a few hundreds of mV after the voltammetric peak, the eigenfrequency of the quartz crystal shows a steep decrease, but which cannot definitely be attributed to mass uptake on the surface : indeed, the equivalent resistance DR of the quartz crystal simultaneously increases to several MW, indicating that considerable viscoelastic losses are occuring within the (viscous) coating which is being deposited on the surface. This feature was attributed to the gelification and/or the precipitation of the incompletely swollen polymer coming from the solution [11]. Since this gelification and/or precipitation is occuring at electrode potentials more cathodic than the above rigid zone, one can conclude that the gelified and/or precipitated polymer is deposited on the surface after the grafted film is formed, *i.e.* it is deposited on the grafted film, as Fig. 3 suggested.

This short list of qualitative arguments strongly argues in favour of a grafted polymer being formed directly on the surface of the metallic electrode. An overall - probably simplistic - picture of electropolymerized layers is that of « hairs » of polymer chains, one portion of which are chemically grafted on the surface, the other chains being entangled in the grafted brush (Fig. 6).

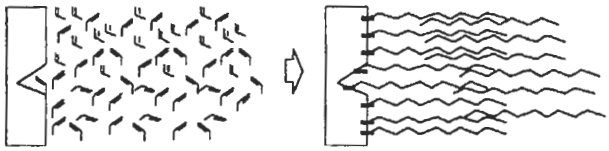

Figure 6 Artist's view of the electrografting process, highlighting the size of the starting molecules (the monomers), and the presumed ideal arrangement of both the grafted chains and the entangled non grafted chains.

Whatever the actual grafting ratio (*i.e.* the proportion of surface sites occupied by a polymer chain), our electropolymerized layers show very original properties, which would all be in line with the occurrence of the grafted layer, i.e. with the fact that metallic surface atoms are involved in chemical bonds with the grafted polymer [12].

First, the occupation of the metallic surface sites by grafted chains is the source of a strong barrier effect against corrosion. Fig.7 shows a picture of ordinary steel protected by a 40 μm film of PolyAcryloNitrile (PAN) on the right side, and left in deaerated sea water for 1 month. The protection achieved by this layer is all the more striking as more than 300 μm are needed to get the same result with traditional varnishes, and as PAN is not precisely known for his intrinsic barrier virtues against corrosion. Even the more severe test of impedance spectroscopy reveals that the PAN film constitutes a quasi ideal capacitor over the whole frequency domain (Fig. 8). Note that the low ca-

Figure 7. Picture of a steel coupon partly coated with a 40 μm thick film of PAN, and left in aerated sea water for one month (magnification x10).

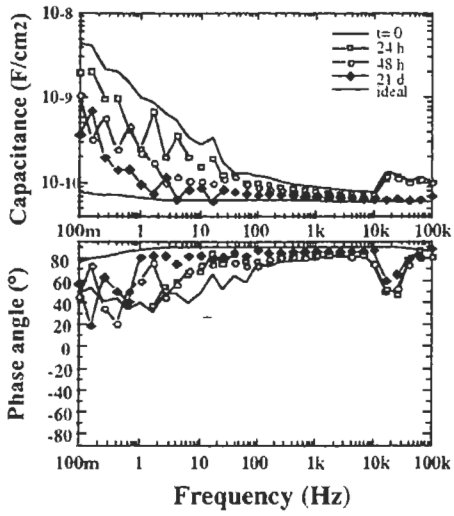

Figure 8 Impedance spectroscopy diagrams of a PMAN film, giving the capacity (top) and the phase angle (bottom) as a function of excitating frequency. Measurements are performed in water at various ages of the film (t=0, 24 h, 48 h and 21 days). The solid line (low and constant capacity, phase angle = 90°) is the behaviour of an ideally protecting capacitor.

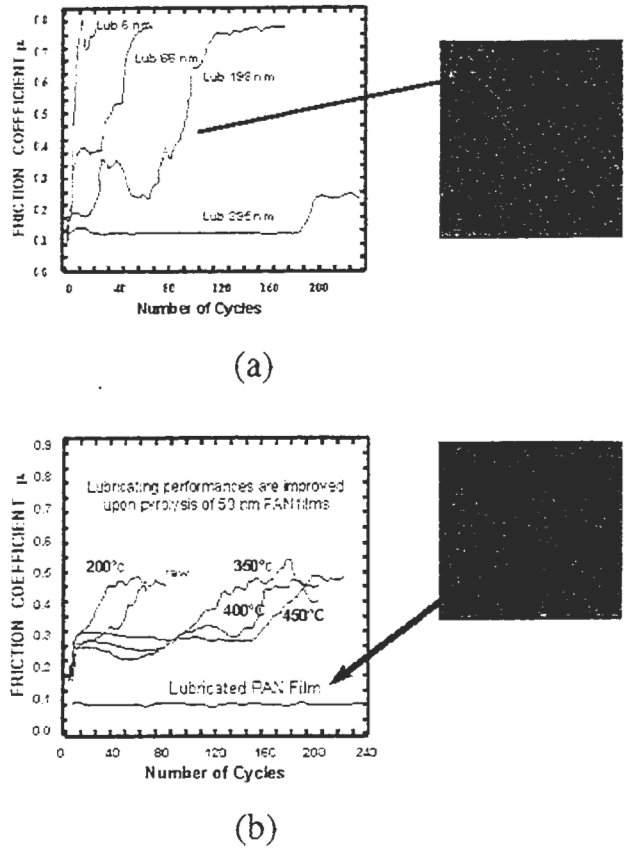

Figure 9 (a) Friction coefficient as a function of the number of cycles for a golden ball sliding on a gold surface (pressure : 50 gf) covered with layers of commercial PerFluoroPolyEther lubricants. The picture on the right is a x50 view of the track region after 100 cycles on the 198 nm thick sample.
(b) Friction coefficient as a function of the number of cycles for a golden ball sliding on a gold surface (pressure : 50 gf) covered with a 50 nm PAN film pyrolyzed at various temperatures (resulting thickness = 50 nm). The same quatity is also shown for a lubricated PAN film (450°C PAN + PFPE). The picture on the right is a x50 view of the track region after 220 cycles on the lubricated PAN film sample.

pacitance measured in the low frequency domain actually is an artifact, stemming from the paramount capacitance of the sample, which is not adapted to the one of the impedance-meter, rather than to a true deficiency.

Second, when a PerFluoro-PolyEther (PFPE), traditionally used for lubrication on gold contacts in microelectronics, is deposited on a pyrolyzed PAN film, considerable improvements are obtained as to the tribological properties of the assembly. Fig. 9a shows that for a golden ball sliding on a gold surface (pressure : 50 gf) covered with about 200 nm of PFPE, the polymer layer is wiped out from the sliding zone after 80 cycles, leaving the two metallic surfaces in contact, with a resulting high friction coefficient between them. In Fig. 9b, the sliding zone of a layer made of 50 nm of pyrolyzed grafted PAN + 100 nm PFPE is still essentially intact after 250 cycles. More importantly, Fig. 9b shows that the PFPE lubricant was not evacuated from the sliding zone. Due to the strong adhesion of the PAN layer, the sliding of the ball actually occurs in between the PFPE and the pyrolyzed PAN film, and not directly on the metallic surface. In addition, Fig. 10 shows than under a pressure of 50 gf on the ball, the contact resistance of the pyrolyzed PAN+PFPE assembly is still of the order of 5 mW, *i.e.* about the same as genuine golden contacts. This feature is due to the PAN film, which is changed from an insulator to a semi-metal upon pyrolysis, ultimately leading to carbon fiber [12].

2. On the grafting mechanism : tracking transcient surface species

Eventhough the above arguments tend to focus onto the same suggestion of a surface polymerization, deeper insights have been conducted in order to understand the reaction mechanism leading to the grafted polymer. One of the main difficulty was to try and « separate » the mechanism leading to the physisorbed polymer from that giving the grafted one.

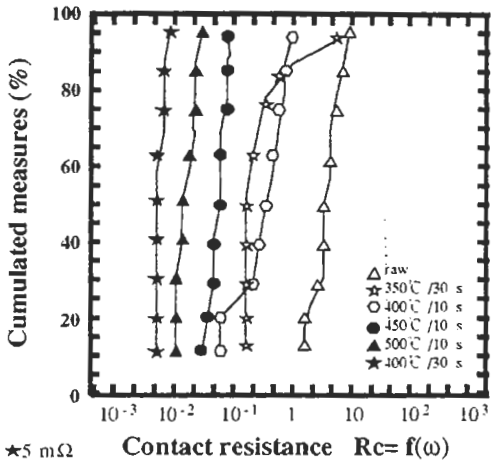

Figure 10 Cumulated measures of the contact resistance of PAN films, using the same device and experimental as the one used for the friction coefficients measurements. The best results are obtained for a PAN film pyrolyzed for 30 s at 400°C, for which the contact resistance is 5 mW, *i.e.* the same as with a gold contact.

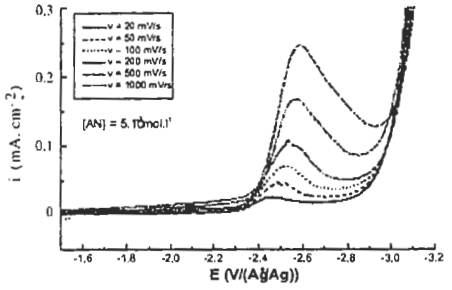

Figure 11 Series of voltammograms giving the measured electrochemical current as a function of the voltage applied to the working electrode (with respect to a reference silver electrode), for a 5.10^{-3} mol.dm^{-3} solution of acrylonitrile in acetonitrile. The electrode potential is imposed linearly from –1.5 to –3.1 V/(Ag$^+$/Ag), at scan rates varying from 20 to 1000 mV/s (see insert).

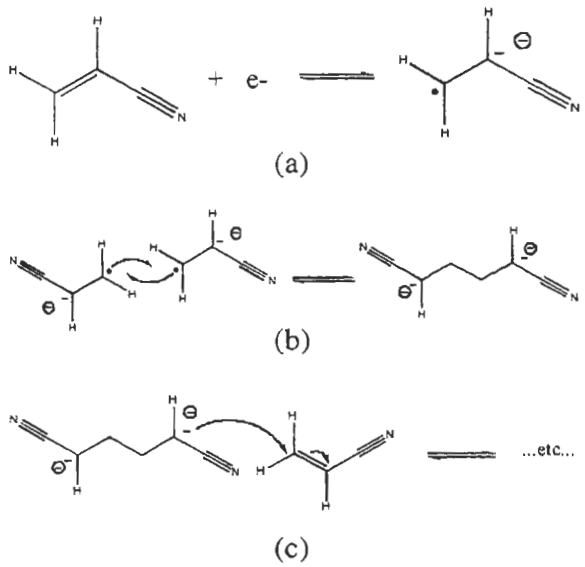

Figure 12 Reaction mechanism accounting for the formation of the polymer film formed in solution (on the instance of acrylonitrile), and comprising : (a) the reduction of the monomer to form the radical anion, (b) the dimerization of the radical anion to form a bi-functional initiator, and (c) the propagation reaction in solution.

This turns out to be rather a difficult task. At low concentration in AN, the voltammetric i(V) curves recorded during the synthesis (giving the current as a function of the applied electrode potential) show a single, so-called diffusion, peak (Fig. 11). This peak features the reduction of AN into its radical anion (Fig. 12a). As the concentration is raised, the voltammogram becomes much more complex, and contains at least two non-diffusional peaks (Fig. 13). The interpretation of the shape of this voltammogram is still debated, but it most probably stems from a « regular » peak enveloppe (such as those obtained at low concentration), in which a depletion is formed (Fig. 13). Our opinion is that this depletion is caused by the abundant consumption of the monomer in the vicinity of the metallic surface because of the polymerization in solution (Figs. 12b-12c). One can note that the polymerization which occurs in solution has a kinetics which is of second order with respect to the concentration in monomer : it is thus faster as the concentration is increased (Fig. 12b). Accordingly, as this reaction abundantly consumes monomer molecules, these are prevented from being reduced and hence from contributing to the current, which leads to an early peak. This hypothesis is qualitatively supported by recent numerical simulation of voltammograms, obtained by solving the partial differential equations of diffusion in the presence of a coupled polymerization [13]. In short, this interpretation of Fig. 12 leads to the conclusion that, as soon as the concentration in monomer is high enough for the polymerization in solution to be active, this polymerization is the overwhelmingly major phenomenon, and thus prevents the direct study of the sole grafting reaction.

In between the above two, high and low, concentration domains, however, we have noticed that apparently conventional (one peak) voltammograms could be obtained, although the peak is not of a purely diffusional character anymore (Fig. 14). As shown in Fig. 14, the convolved current I(V) (easily computed from the experimental i(V) [14]) exhibits a maximum : this feature, seldom encountered,

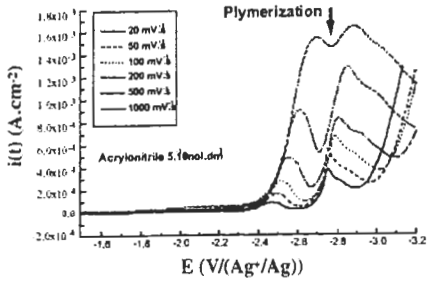

Figure 13 Series of voltammograms for a 5.10^{-2} mol.dm^{-3} solution of acrylonitrile in acetonitrile, illustrating the appearance of multi-peak curves, most probably stemming from the abundant consumption of the monomer molecules by the coupled polymerization in solution. The electrode potential is imposed linearly from –1.5 to –3.1 V/(Ag$^+$/Ag), at scan rates varying from 20 to 1000 mV/s (see insert).

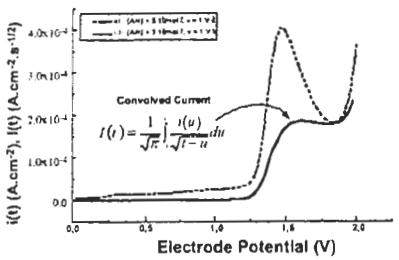

Figure 14 Voltammogram obtained for a 10^{-2} mol.dm^{-3} solution of acrylonitrile in acetonitrile (dashed curve), and corresponding convolved current (solid line) calculated from the raw data, illustrating the fact that the peak current is not purely diffusional, and that adsorption effects are probably involved (occurrence of a maximum on I(t)).

would be a direct proof that the radical anion of AN (Fig. 12a) is actually formed on the surface of the electrode, *i.e.* it is chemisorbed [14]. This suggestion amounts to estimating that the charge transfer reaction is incompletely described by Fig. 12a : one has to replace it by the more detailed picture given by Fig. 15, featuring an adsorbed product of reaction for the charge transfert, redox, reaction.

This proposal raises a certain number of questions, and needs to be detailed.

The radical anion of AN is negatively charged, and as the redox reaction has taken place on a cathode (a surface which is polarized negatively), this anion would be strongly repelled by the surface (Fig. 15). This suggests that this species (if it exists) is highly unstable, and one may wonder whether its introduction is merely relevant to account for the reaction path.

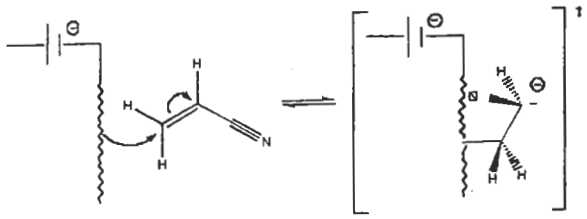

Figura 15 Proposed molecular model detailing that the radical anion is adsorbed – according to experimental findings (see Fig. 14) – and that the charge transfer step is more complex than the simplistic view of Fig. 12a.

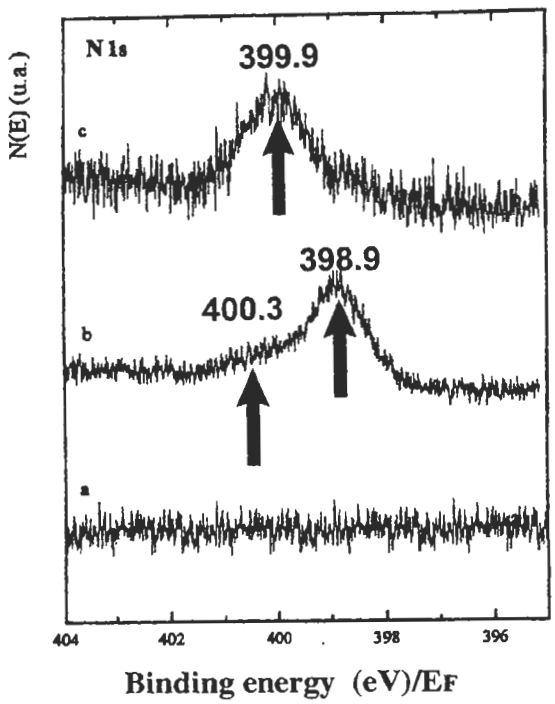

Figure 16 N 1s region of the XPS spectra of : (a) initial copper surface dipped in acetonitrile ; (b) a copper surface submitted to pre-electrolysis for oxide-reduction, and subsequent dipping in acetonitrile ; (c) a copper surface submitted to pre-electrolysis and subsequent dipping into a solution of acrylonitrile in acetonitrile.

Actually, the issues of : (i) the possibility of its being formed on the surface ; and (ii) its lifetime on the surface once it is formed; are intrinsically different matters, and we shall consider them separately. Indeed, Fig. 16 shows the N1s region of the XPS spectra of three different copper electrodes : in Fig. 16a, the copper electrode has been merely dipped into acetonitrile (the solvent), dried and put into the UHV chamber of our ESCA apparatus. It shows

no trace of nitrogenated species. In Fig. 16b, the copper surface has been submitted to electrochemical polarization in the absence of the monomer (pre-electrolysis), rinsed with acetonitrile, and then put under UHV : two N1s lines are obtained, at 398.9 and 400.3 eV, which correspond to chemisorbed acetonitrile molecules [15]. In Fig. 16c, a copper surface is first pre-electrolyzed (solvent only), the polarization is stopped while the electrode is kept in the solvent, and AN is then added dropwise to the solution. The electrode is then rinsed with acetonitrile and put into the UHV chamber. One N1s line is obtained at 399.9 eV, which has been shown to correspond to chemisorbed AN, lying flat on the surface [16]. This shows that neutral AN chemisorbs more readily on metallic Cu than the solvent, and is capable of displacing the adsorbed solvent molecules observed in Fig. 16b. The true reactant in the synthesis is thus chemisorbed neutral AN, lying flat on the surface, rather than a Cu surface in front of free AN molecules : as the charge transfer occurs under Born-Oppenheimer conditions (*i.e.* at fixed positions for the nuclei), the radical anion of AN is thus readily formed chemisorbed on the surface, initially at the geometry of the adsorbed neutral AN molecule [17]. Hence, we recover in a different way the conclusions obtained with the convolved currents (Fig. 14).

The second issue is now to be able too determine the lifetime of this chemisorbed anion on the surface, before it desorbs and eventually goes into the solution. Note that - at this point - the traditional RRC coupling (Figs. 12b-12c) is recovered once the adsorbed radical anion desorbs. This accounts for the polymerization in solution. Our point is now to examine whether the chemisorbed radical anion has sufficient a lifetime to do some surface chemistry before it desorbs, and account for the grafting mechanism (Fig. 17).

3. On the lifetime of the chemisorbed radical anion : a theoretical model

A direct measure of the lifetime of the presumed chemisorbed radical anion, although possible in principle, is presently out of reach. First because it is only presumed, and second because it would involve rather complex experimental procedures, e.g. coupling non-linear optics (such as Sum Frequency Generation) to pico-second time resolution. Work is in progress in our group along these lines, but we only wish here to present some arguments supporting our views.

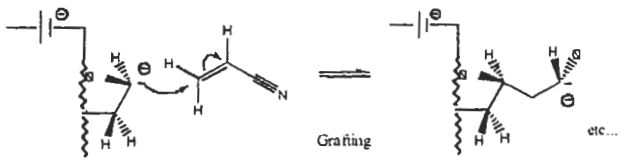

Figure 17 Presumed reaction mechanism accounting for the formation of grafted polymer chains on the electrode.

Our present concern is to be able to determine an order of magnitude of the lifetime t of the chemisorbed radical anion, on the basis of simple, sound but plausible theoretical considerations. We shall then compare t with the characteristic time $(k_p.c)^{-1}$ for the surface polymerization to start (Fig. 17). Indeed, the reaction depicted in Fig. 17 remains relevant as long as $\tau \sim (k_p.c)^{-1}$. If $\tau << (k_p.c)^{-1}$, then the chemisorbed radical anion always desorbs before adding to a fresh monomer molecule, and the mechanism of Fig. 17 is irrelevant.

Making a theoretical evaluation of the lifetime t first amounts to evaluating the effective potential energy hypersurface of the chemisorbed radical anion as a function of its position with respect to the surface : distance, orientation, intramolecular deformation...etc. Once this hypersurface is known, the lifetime can be easily deduced from e.g. a numerical resolution of the time-dependent Schrödinger equation describing the movement of the nuclei on this hypersurface.

In order to simplify the problem, and since a mere order of magnitude is sought for, we have considered a one-dimensional model for our system [17]. Geskin et al. recently published a study in which they modelled the initial stages of the electropolymerization of AN precisely by using an external uniform electric field to simulate the Electrochemical Double Layer (EDL) existing at a polarized copper electrode [18]. They considered a monomer of AN on several Cu_n clusters mimicking the monocristalline Cu(100) surface, using quantum-chemistry based Density Functional Theory calculations. In their model, the whole system is embedded in fields perpendicular to the surface, with intensities ranging from $0.77.10^8$ to $1.03.10^8$ $V.cm^{-1}$. They observe that for higher field strengths, the chemisorbed radical-anion is unstable on the negatively charged surface, in the sense that no bound state could be found when trying to optimize its geometry. More importantly, the dissociation between the molecule and the surface occurs at the carbon/metal chemical bond. As far as the results of ref.[18] are concerned, there seems to be no dissociation of the reduced molecule prior to desorption. Additionally, the internal molecular structure of the chemisorbed radical anion is very similar to that when it has desorbed and is free: the dissociation essentially occurs at frozen internal coordinates for the radical anion [17]. This informa-

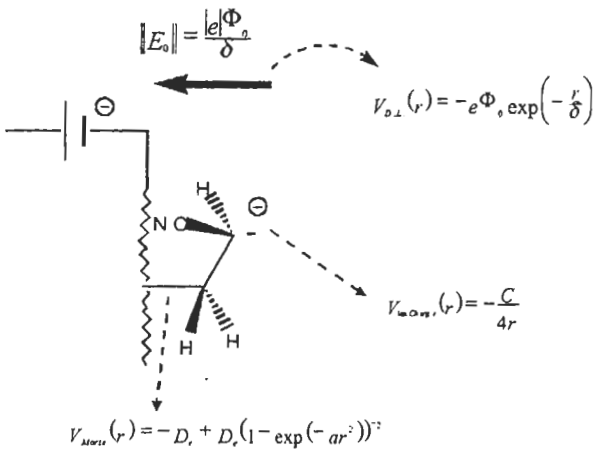

Figure 18 Analytical form of the three contributions to the one-dimensional potential modelling the interaction between the chemisorbed radical anion of Fig. 15 and the polarized metallic surface : $V_{D.L}(r)$, accounting for the effects of both the interfacial double layer electric field and the surrounding solvent, $V_{Im.Charge}(r)$, accounting for the interaction of the negative charge of the radical anion with its image charge within the metal, and $V_{Morse}(r)$, accounting for the carbon/metal interface bond.

tion indicates that one can plausibly model the chemisorbed radical anion by a small sphere, bearing a negative point charge, interacting: (i) with its image charge built within the metal (attractive); (ii) with the electric field present within the EDL (repulsive); and: (iii) attached to the surface by a potential featuring a carbon/metal bond (attractive) (Fig. 18) [17]. In such a model, only the distance of the center of the sphere to the surface plane is then varied, and the effective potential (which is the sum of the three above contribution), is one-dimensional, $V_{eff}(r)$ (Fig. 18) [17].

The next step is to have functional forms for each of the three above contribution to the global effective potential, *i.e.* to exhibit parametrized functions, and connect their parameters with experiment. This can be achieved pretty easily for contributions (i) and (iii), which describe the image charge and the interface chemical bond, respectively [17]. This is more difficult for term (ii), which requires that a functional relation be found between the experimental electrode potential (which is a macroscopic quantity, in Volts) and the electric field within the EDL (which is a microscopic quantity, in $V.cm^{-1}$).

4. Calibrating the repulsive term using the Stark-Tuning effect

Such a calibration of the repulsive potential has been performed by comparing theory with experiment on the description of the Stark-Tuning effect of CO on Pd(100) [17]. The experiments carried out e.g. by Zou et al. describe a Pd(100) electrode, covered with CO and polarized in solution [19]. Simultaneously, the C-O and Pd-C stretching vibrational frequencies are recorded using Surface Enhanced Raman Spectroscopy (SERS) as a function of potential, $\nu_{CO} = f(V)$, $\nu_{PdC} = g(V)$. The variations of these vibrational frequencies has been interpreted as stemming from the interaction of the dipole moment of CO with the electric field within the EDL, and were thus referred to as the Stark-Tuning effect [20].

We were particularly interested in these experiments, because they are a direct way to probe the electric field within an EDL: CO is a small molecule, which should be completely embedded in the EDL. Moreover, a fully ab initio theoretical estimation of this Stark-Tuning effect can be carried out. Using Density Functional Theory, we have computed how the C-O and Pd-C stretching frequencies of a CO molecule adsorbed on Pd(100) clusters, vary as a function of an applied electric field $\mathbf{E}_0$ perpendicular to the cluster surface (Fig. 19) [17]. These calculations thus deliver $\nu_{CO} = f'(\mathbf{E}_0)$, $\nu_{PdC} = g'(\mathbf{E}_0)$, i.e. an estimation of the variations of the stretching frequencies as a function of the interfacial electric field.

One thus sees that comparing theory with experiment affords an implicit relationship between the electrode potential V and the electric field within the EDL, $\mathbf{E}_0$. It turns out that the experimental $\nu_{CO} = f(V)$ and $\nu_{PdC} = g(V)$ curves are straight lines [19]. The same is true for our theoretical $\nu_{CO} = f'(\mathbf{E}_0)$, $\nu_{PdC} = g'(\mathbf{E}_0)$ curves, so that - ultimately - the relationship between V and $\mathbf{E}_0$ can be made explicit, and is

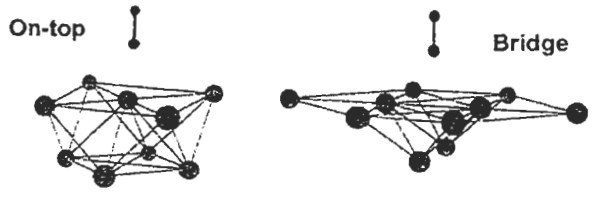

Figure 19. Molecular structure of the Pd_9CO and $Pd_{10}CO$ clusters used to compute the effect of an applied uniform electric field on the vibrational frequency of adsorbed CO, using quantum chemistry. The results of these calculations, when compared to the corresponding experimental measurements by SERS, afford a calibration of $V_{D.L}$ (Fig. 18), i.e. of the interfacial electric field under polarization in solution.

linear [17]. A comparison between theory and experiment reveals that the coefficient of proportionality, or so called electric field rate (in $(V.cm^{-1}).V^{-1}$), is given by an equation of the type :

$$\rho_{E0} = a \, . \, z \, . \, (C_0/\varepsilon)^{1/2}$$

where $a = 2.91.10^8$ for ρ_{E0} to be given in $(V.cm^{-1}).V^{-1}$, z is the charge of the ions of the (symmetric, z:z) supporting electrolyte, C_0 is the concentration in the supporting electrolyte, and ε is the permittivity of the solvent [17]. The validity of this equation is pretty much connected to that of the Gouy-Chapmann equation [21], which is used to describe the underlying structure of the EDL [17], and is thus restricted to low concentrations in the supporting electrolyte. For a solution containing a (1:1) electrolyte at a 0.1 M ionic strength in water (ε =78.5), the predicted electric field rate is thus $1.04.10^7$ $(V.cm^{-1}).V^{-1}$. Note that this value is pretty close to the one proposed by Bockris et al., namely $(2.9\pm0.3).10^7$ $(V.cm^{-1}).V^{-1}$ [22].

5. Chemisorbed radical anions : incidences of a non-zero lifetime

Our experiments are carried out in acetonitrile (e = 36), using a (1:1) supporting electrolyte (Tetra Ethyl Ammonium Perchlorate, TEAP, $(CH_3CH_2)_4N^+$, ClO_4^-), at a concentration of the order of 0.1 M. Thus, for an electrode potential of the order of 1 Volt apart from the Potential of Zero Charge (PZC), one is always in a situation where $E_0 \sim 10^7$ $V.cm^{-1}$, or anyway $E_0 < 10^8$ $V.cm^{-1}$ largely.

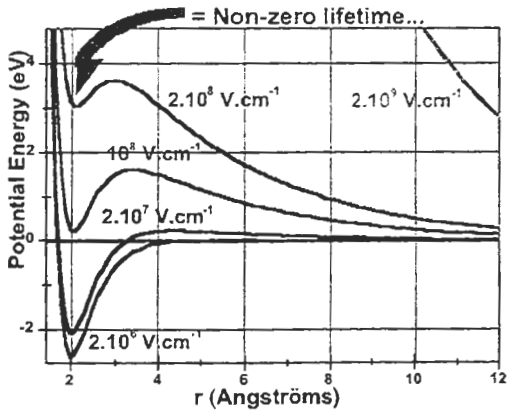

Figure 20 Series of curves giving the effective potential seen by the chemisorbed radical anion (sum of the three terms of Fig. 18), as a function of distance with respect to the surface, for various repulsive electric field strengths at the interface. The potential is fully repulsive at E = 2.10^9 V/m. It is still repulsive at E > 2.10^7 V/m, but the emergence of a well at ρ = 2 Å insures that the lifetime of the radical anion on the surface is finite at such fields.

Fig. 20 shows a plot of the effective potential, $V_{eff}(r)$, felt by our model charged sphere (Fig. 18) as a function of distance r, for several electric field strenghts [17]. One sees that in between high field strengths, say higher than 10^9 $V.cm^{-1}$ where the potential is uniformly repulsive (= lifetime is zero), and low field strengths, lower than about 10^6 $V.cm^{-1}$ where the potential is that of a bound state (= lifetime is infinite), a new family of curves is obtained. For fields of the order of 10^7-10^8 $V.cm^{-1}$, the effective potential is - on the whole - repulsive, but contains a well in the vicinity of the surface (and stemming mainly from the image charge potential) (Fig. 20). Such a well is synonymous with a non-zero lifetime for the charged sphere, and hence for the chemisorbed radical anion on the polarized surface [17].

Returning back to our questions of section 2, we may now say that the hypothesis of a chemisorbed radical anion is mandatory. The issue as to whether this compound is capable of accounting for the grafted films is still unresolved, since it amounts to calculating and (if possible) measuring its lifetime on the surface. What can be said at present is that this lifetime is not equal to zero, and that this hypothesis remains highly plausible.

Let us now stress that the lifetime of the first chemisorbed radical anion is the only one we have to consider to assess the grafting mechanism. Indeed, if one imagines that proper conditions for grafting are fulfilled ($t \sim (k_p.c)^{-1}$), then the reaction depicted in Fig. 17 may occur, leading to a dimeric chemisorbed radical anion. However, upon dimerization, the anionic charge (which is essentially on the edge carbon) is suddenly moved away from the surface by about 10 Å (the edge-to-edge size of an AN molecule), as far as it may go since it is repelled by the polarized metallic surface (Fig. 17). At this point, the charge/surface Coulombic repulsion is abruptly lowered, and the intrinsic instability of the grafted organics suddenly disappears : the dimerization involving the chemisorbed radical anion stabilizes the overall chemisorbed structure, which is then ready for further addition to another fresh AN molecule.

6. Characterization of the products of reaction : surface analysis

There are two very significant consequences of the mechanism depicted in Fig. 17: (i) at least for the monomeric and dimeric chemisorbed radical anions - the structure is embedded in the electric field of the EDL, which is approximately perpendicular to the surface. One may thus expect a strong preferential orientation of the polymer

chains, one should find the footprint of at the end of the synthesis; (ii) as suggested by the arguments listed in the introduction, a chemical interface bond is expected between the grafted chains and the metallic surface. Fig. 17 shows that this bond is simply that through which the monomeric radical anion remained chemisorbed (Fig. 18) before initiating the grafted polymerization. It is thus also a frozen footprint of the initial steps of reaction.

Both features, (i) and (ii), have been evidenced experimentally.

Fig. 21 shows the XANES spectra of a PAN film, taken at the carbon and nitrogen K edges both at normal and grazing angle with a polarized incident X-ray beam from a synchrotron source [23]. XANES is an absorption spectroscopy, in which an electron coming from a core level (the C1s and N1s in the present case) is excited to the Lowest Unoccupied Molecular Orbital (LUMO). Quantum chemistry calculations show that for PAN, the LUMO is located essentially on the p system of the CN groups [24]. Hence, if the polymer chains are oriented in any specific way with respect to the surface, so will be the CN groups attached to them, and one then expects different signal intensities from the grazing and normal incidence beams. As is seen in Fig. 21, this is actually the case [23].

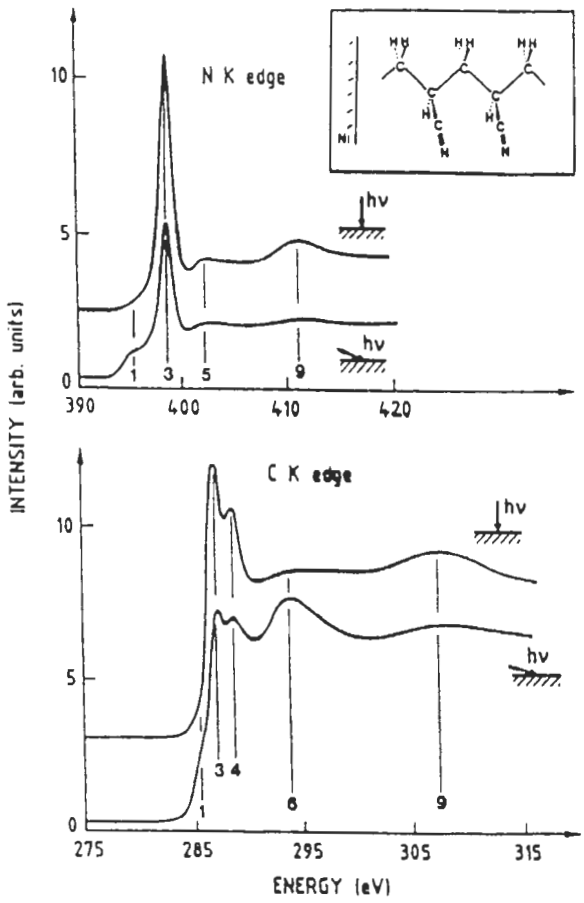

Figure 21 XANES spectra of a PAN film at normal and grazing incidence, both at the N (top) and C (bottom) K edge.

Let us now turn onto the interface bond: Fig. 22 shows the C 1s region of the XPS spectra of various nickel surfaces [5]: (a) the initial nickel surface, showing hydrocarbon and carboxylate contamination; (b) a nickel surface covered with a thick (> 500 Å) PMAN film obtained by electropolymerization; the corresponding spectrum locates the two lines characteristic of PMAN; and: (c) a nickel surface covered with an ultra-thin PMAN film (≈ 20 Å by ellipsometry); in this last spectrum, one identifies the lines encountered both in samples (a) and (b), plus one additional component located at 283.6 eV, i.e. compatible with a carbon/metal bond [5]. Preliminary theoretical calculation on model molecules mimicking a grafted monomer

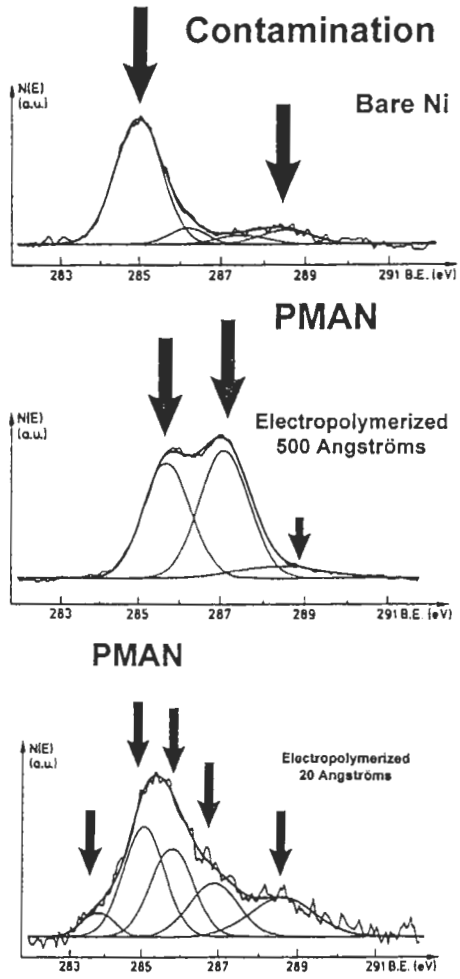

Figure 22 C 1s region of the XPS spectra of: (i) the initial bare Ni surface (top); (ii) a Ni surface covered with an electropolymerized PMAN film of 500 Å; (iii) a Ni surface covered with an electropolymerized film of 20 Å, and enabling an evidencing of interfacial carbon/metal bonds.

and a grafted dimer, have given a predicted C 1s chemical shift around 283.8 eV on a bound state bearing a C/metal chemical bond [25,26].

In order to confirm this attribution on a sounder basis, we have developped a method of calculation, based on quantum chemistry, which enables the highly accurate computation of Core-Electron Binding Energies (CEBEs). This method, which is based on a generalization of the Transition State approach of Slater, makes use of Density Functional Theory [27]. We have recently adapted it to the evaluation of CEBEs for molecules chemisorbed on surfaces [28]. This approach is presented with many more details in another paper of these proceedings, and feature articles may also be found elsewhere [29].

7. Concluding remarks

This paper constitutes a brief review of our contribution to the study of electrochemical grafting. Thanks to the electrolysis of polymerizable monomers in an organic medium, we are capable of making « hairs » of polymer grow on the surface of conducting materials. The building of true chemical bonds between the polymer and the metal constitutes the key point of our synthesis. New physico-chemical properties obviously stem from these interfacial bonds, some of which may find definite use in applied fields such as anti-corrosion, lubrication, adhesion, biocompatibilization...etc.

However, while these physico-chemical properties are obvious at a macroscopic scale, the full characterization of the interfacial molecular structures is still a difficult and non totally resolved task. As one studies the sole product of reaction i.e. the grafted polymer, one is faced with the problem of burried interfaces, very few surface-sensitive techniques can nowadays cope with. As one is interested in the true reaction paths, i.e. the time-resolved building of the grafted film, one is faced with the problem of transcient species having very short lifetimes.

Both these difficulties point to the fact that only surface-sensitive techniques are nowadays available to the surface chemist, and that true interface-sensitive techniques are either lacking or difficult to adapt for routine use. New experiments are being attempted in our group along these lines. However, we have also found it peculiarly useful to examine what theoretical models can bring. Quantum chemistry calculations have now reached a high degree of quality and speed, which enables one to think of them as a true piece of information, particularly when the corresponding experiments are not easy to carry out. We have given here the example of the calculation of XPS chemical shifts, which can nowadays be predicted with an accuracy of about 0.2 eV using Density Functional Theory (DFT). In our case, DFT calculations have also been used to evaluate the lifetime of transcient chemisorbed species, and argue in favour of a mechanism involving surface chemical reactions. Much can be taken out from theoretical models, considered as a mere piece of information, no more no less. Having a very accurate method of calculation at hand is e.g. amply sufficient to increase the accuracy of an XPS apparatus at - almost - no cost, since most of these calculations can be performed on personal computers. In this respect, we think that this « theoretical complement » may find its place even in the industry.

References

[1] (a) G. Lécayon, Y. Bouizem, C. Le Gressus, C. Reynaud, C. Boiziau, and C. Juret, Chem. Phys. Lett., **91**, 506 (1982). (b) C. Boiziau, G. Lécayon, Surf. Interf. Analysis, 12 (1988).

[2] (a) G. Deniau, G. Lécayon, C. Bureau and J. Tanguy, in, Y. Pauleau and P.B. Barna (Eds.), Protective coatings and Thin Films, Kluwer Academic Publishers, 1997, p.265. (b) G. Deniau, C. Bureau and G. Lécayon, submitted.

[3] C.Doneux, R.Caudano, J.Delhalle, E.Léonard-Stibbe, J.Charlier, C.Bureau, J.Tanguy and G.Lécayon, Langmuir, **13**, 4898 (1997).

[4] G. Deniau, N. Huet and C. Bureau, in preparation.

[5] (a) G. Deniau, P. Viel and G. Lécayon, Surf. Interf. Anal., **18**, 443 (1992) . (b) C. Bureau, M. Defranceschi, J. Delhalle, G. Deniau, J. Tanguy, G. Lécayon, Surf. Sci., **311**, 349 (1994). (c) C. Bureau, G. Deniau, F. Valin, M. G. Guittet, G. Lécayon and J. Delhalle, Surf. Sci., **355**, 177 (1996).

[6] P. Newton, private communication.

[7] P. Viel, C. Bureau and G. Lécayon, submitted to J. Electroanal. Chem.

[8] J. Tanguy, G. Deniau, G. Zalczer and G. Lécayon, J. Electroanal. Chem., **417**, 175 (1996).

[9] C. Doneux, Ph.D Thesis, Facultés Universitaires Notre-Dame de la Paix, Namur, Belgium (1998).

[10] G. Sauerbrey, Z.Phys., **178** (1964) 457.

[11] J. Charlier, C. Bureau and G. Lécayon, submitted to J. Electroanal.Chem.

[12] (a) S. Noel, P. Newton, C. Bodin, F. Houzé, L. Boyer, P. Viel, F. Valin and G. Lécayon, Surf. Interf. Anal., **22**, 393 (1994). (b) F. Houzé, L. Boyer, S. Noel, P. Viel, G. Lécayon and J.M. Bourrin, Synth. Metals, **62**, 207 (1994).

[13] C. Bureau and L. Quiv, submitted to J. Electroanal.

Chem.
[14] M.O. Bernard, C. Bureau, J.M. Soudan and G. Lécayon, J. Electroanal. Chem., **431**, 153 (1997).
[15] C. Bureau and D.P. Chong, Chem. Phys. Lett., **264**, 186 (1997).
[16] C. Bureau and X. Crispin, in preparation.
[17] C. Bureau, S. Kranias, X. Crispin and J.L. Brédas, submitted to Prog.Theor.Chem.
[18] V. M. Geskin, R. Lazzaroni, M. Mertens, and R. Jérôme, J.Chem.Phys., **105**, 3278 (1996).
[19] S. Zou, and J. M. Weaver, J.Chem.Phys., **100**, 4237 (1996).
[20] M. Head-Gordon, and J.C. Tully, Chem.Phys., **175**, 37 (1993).
[21] A. J. Bard and L. R. Faulkner, Electrochemical Methods (John Wiley & Sons, New-York, 1980).
[22] J. O'M. Bockris, M. A. V. Devanathan and K. Muller, Proc.Roy.Soc.London Ser.A, **274**, 55 (1962).
[23] G. Tourillon, R. Garrett, N. Lazarz, M. Raynaud, C. Reynaud, G. Lécayon and P.Viel, J. Electrochem. Soc., **137**, 2499 (1990).
[24] G. Deniau, G. Lécayon, P. Viel, G. Hennico and J. Delhalle, Langmuir, **8**, 267 (1992).
[25] C. Bureau, Ph.D Thesis, Université Paris VI (1994).
[26] C. Bureau, M. Defranceschi, J. Delhalle, G. Deniau, J. Tanguy and G. Lécayon, Surf. Sci., **311**, 349 (1994).
[27] D.P. Chong, Chem.Phys.Lett., **232**, 486 (1995).
[28] C. Bureau, Chem.Phys.Lett., **269**, 378 (1997).
[29] C. Bureau, D.P. Chong, J. Delhalle, K. Endo, G. Lécayon and A. Le Moel, Nucl. Instr. Meth. Phys. Res. B, **131**, 1 (1997).